The Reilly Peak Tertiary(?) intrusive--A high-silica rhyolite

Linda Lee Davis, 1986, pp. 167-171

in:

Truth or Consequences Region, Clemons, R. E.; King, W. E.; Mack, G. H.; Zidek, J.; [eds.], New Mexico Geological Society 37th Annual Fall Field Conference Guidebook, 317 p.

This page is intentionally left blank to maintain order of facing pages.

THE REILLY PEAK TERTIARY(?) INTRUSIVE—A HIGH-SILICA RHYOLITE

LINDA LEE DAVIS
Department of Geology, University of Georgia, Athens, GA 30602

Abstract—Paleozoic sedimentary rocks at Reilly Peak are intruded by a high-silica intrusive rhyolite, felsic dikes, and mafic dikes. An extensive fracture system and skarn are developed in the sedimentary and igneous rocks. Breccia pipes are common. Textures in the intrusive rhyolite range from nearly 95% spherulitic to trachytic. Felty intergrowths of feldspar and cristobalite(?), granophyric and glomeroporphyritic quartz and feldspar, and micropoikilitic quartz commonly envelope the spherulites, and are also present where spherulites are not developed. Trachytic textures are common near the margins of the intrusive and in its northern extension, which is a sill or dike. Fibrous biotite, epidote, and titanite are interstitial to spherulites and appear to have grown after their development. Microphenocrysts of plagioclase (Ab_{95-97}) and lath-like biotite, and resorbed quartz are in the cores of the spherulites. This implies that they crystallized before or during spherulite growth. Alteration of the intrusive is represented by the kaolinite, sericite, and biotite. Microprobe analyses of biotites from several localities within the intrusive indicate varying degrees of hydrothermal alteration throughout the stock and sill. The biotites in each sample are significantly different from biotites in other samples. Two biotite species per sample can be distinguished on the basis of morphology, relative analytical totals, number of Si ions/unit cell, and sometimes by K_2O% and CaO%. H_2O and CaO have been added to, and K_2O and SiO_2 removed from, both biotites. The fluids that altered the intrusive rocks are probably the same fluids that formed the skarn at Reilly Peak and Iron Mountain.

INTRODUCTION

Reilly Peak is approximately 8 km north of Winston, New Mexico (inset, Fig. 1), in Sierra County. The peak is almost 275 m higher than the pediment at the base (western flank) and is part of the Sierra Cuchillos.

The Reilly Peak intrusive is part of a system which includes felsic dikes, breccia pipes, an extensive tetrahedral fracture system, healed fractures, and a granitic intrusive at depth. This system is very similar to the hypothetical granodioritic porphyry emplaced in a subvolcanic environment discussed at length by Burnham (1979). Lowell & Guilbert (1970) and Gustafson & Hunt (1975) also described similar systems. Burnham (1979) suggested that the shallowness of emplacement, the presence of breccia pipes, and other geologic features of such systems may indicate solidification of the magma in or near volcanic conduits during the waning stages of volcanic activity. The processes that led to the crystallization of the intrusives, the development of skarn, and alteration of the intrusives are not well known or well studied.

A high-silica-rhyolite intrusive, porphyritic-rhyolite dikes, and mafic dikes intrude Paleozoic sedimentary rocks. Only Paleozoic limestones and the Permian Abo Formation are shown in Fig. 1. The sedimentary rocks at Reilly Peak, aside from the Abo Formation, remain undivided. Stratigraphic sections measured at Iron Mountain, to the north, and at Red Hill Pass (Jahns et al. 1978), a few kilometers to the south, indicate that Cambrian, Ordovician, Devonian, Mississippian, Pennsylvanian, Permian, and Cretaceous sedimentary rocks (limestones, shales, and sandstones) are present.

Porphyritic-rhyolite dikes are found throughout the northern Sierra Cuchillo transecting all lithologies except mafic dikes. Megacrysts of resorbed plagioclase, microcline perthite, and quartz are present along with biotite, epidote, chlorite, apatite, opaques, zircon, and cassiterite(?). Many quartz megacrysts may be xenocrysts. The feldspars display rapakivi texture and the groundmass is fine-grained granophyric. All basaltic dikes and fault wedges of lithic andesitic tuffs are found along or parallel to the western border fault except one (Fig. 1, dike labeled Tib near sample locality 17). These rocks are strongly propylitized (calcite + chlorite + epidote), but original textures can be discerned and some unaltered plagioclase and pyroxene are present. The mafic dikes may be much younger than the intrusive and felsic dikes. Skarn is developed at the contacts between intrusive rocks and limestones. Both endo- and exoskarn are present and are similar mineralogically and chemically to the Iron Mountain skarn a few kilometers north in the same range.

Jahns (1944a, b) described the skarn/tactite at Iron Mountain and Reilly Peak in detail. He divided the metamorphosed rocks into two zones: a zone of simple recrystallization with very little addition of material; and a zone of recrystallization and metasomatism with appreciable addition of material from outside sources. The metasomatically altered rocks are further divided into iron-poor silicate rocks and iron-rich silicate rocks. At Reilly Peak, hornfels, quartzites, and marbles make up the zone of simple recrystallization, and the metasomatized, recrystallized rocks are iron-poor granulites, massive skarn, and "ribbon rock." Endoskarn is restricted to the margins of the intrusives.

This paper presents a description of the fine-grained intrusive at Reilly Peak. It is a progress report aimed at understanding the genesis of the intrusives and development of skarn at Reilly Peak and Iron Mountain. It is suggested that the high-silica rhyolite intruded the sedimentary rocks as did the dikes and sills(?), forming a favorable environment for later fluids to produce alteration assemblages including skarn.

PREVIOUS WORK

The Iron Mountain district has attracted much attention since 1880 when T.K. Scales reportedly shipped a few tons of oxidized lead–copper ore from the southern part of the district (Jahns 1944a). Smythe (1921), Lasky (1932), and Harley (1934) briefly described the stratigraphy, intrusives, and contact-metamorphic deposits of the district. Strock (1941) noted the district as a new helvite locality, the fourth reported occurrence in the United States. Jahns (1944a, b, 1955) thoroughly described the sedimentary, volcanic, and intrusive rocks as well as the tactite and the structural history of the northern Sierra Cuchillos. Kelley (1955) compiled a geologic map of the Sierra County region for the Sixth Field Conference of the New Mexico Geological Society. Alminas et al. (1975a, b, c) published maps showing anomalous distribution of W, Ag, Pb, Sn, Bi, Mo, Cu, Zn, and fluorite. Jahns et al. (1978) revised the stratigraphy of the study area and described the Cenozoic volcanic rocks as well. Correa (1980) discussed fluorine and lithophile element mineralization in the Sierra Cuchillos. Heyl et al. (in preparation) mapped the Iron Mountain quadrangle.

PETROGRAPHY AND GEOCHEMISTRY

The fine-grained, shallow intrusive at Reilly Peak has been described as an extremely fine-grained, homogeneous, white to pearl-gray monzonite (Jahns 1944a). Detailed petrography and chemical analyses show that the intrusive is a high-silica rhyolite. A representative chemical analysis in wt% is as follows: SiO_2, 75.31; TiO_2, 0.08; Al_2O_3, 13.81; Fe_2O_3, 0.79; MnO, 0.02; MgO, 0.19; CaO, 0.78; Na_2O, 3.74; K_2O, 4.07; P_2O_5, 0.05; F, 0.02; Cl, 0.01; L.O.I., 0.84. Textures range from

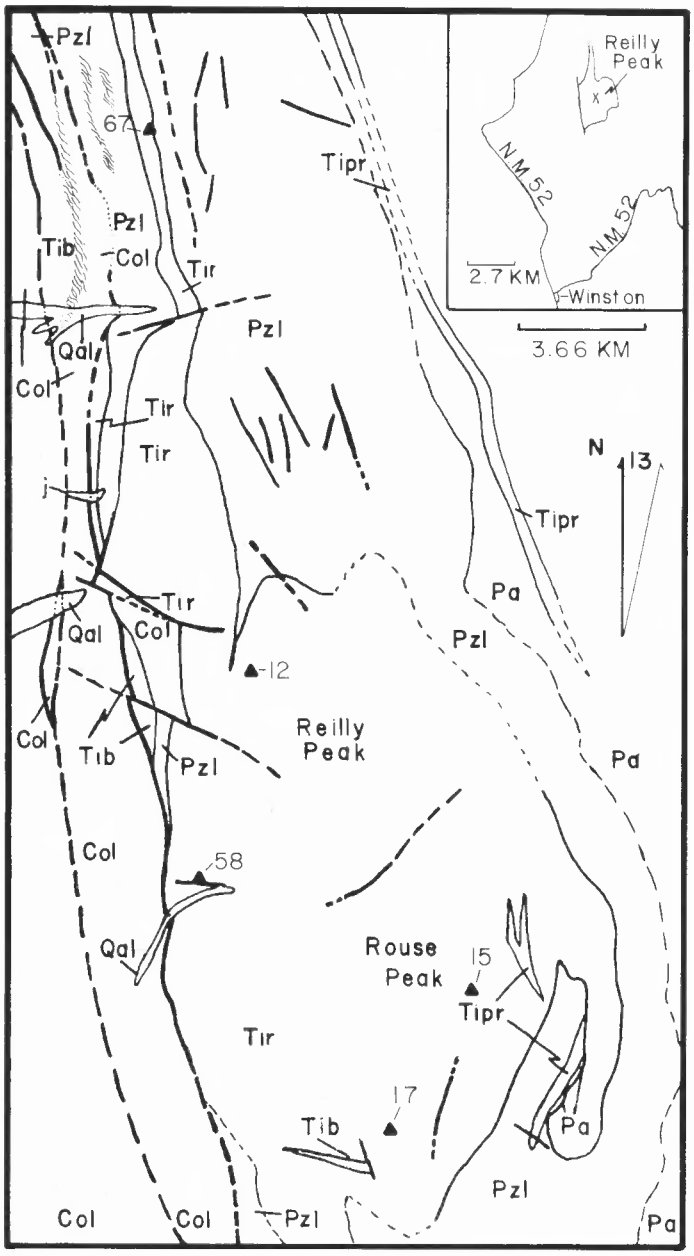

FIGURE 1—Geologic map (Davis, M.S. thesis, in preparation) of Reilly Peak area. Qal = Quaternary alluvium; Col = colluvium; Tir = rhyolite; Tipr = porphyritic rhyolite; Tib = basaltic/andesitic; Pa = Abo Formation; Pzl = Paleozoic limestone, shale, dolomite, and sandstone undivided; j = jasperoid; flattened s symbol represents fault zones.

spherulitic to trachytic (Fig. 2). Many samples show 30–95% spherulitic crystallization with interstitial biotite, epidote, and micropoikilitic quartz. Spherulites are enveloped by felty, felsic intergrowths, or granophyric quartz and albite, or micropoikilitic quartz (Lofgren 1971).

A variety of minor mineral constituents is present. A few percent (1–4%) albite microphenocrysts are common. Biotite, titanite, epidote-group minerals, muscovite/sericite/kaolinite, hematite, Mg-rich calciferous amphibole, apatite, and magnetite are accessory phases. Grain size is rarely larger than 1.0 mm. Phenocrysts of albite, biotite, and epidote are the only phases to reach this size. Glomeroporphyritic albite and quartz (as large as 0.4 mm) are common. Grain boundaries are generally sutured within these intergrowths, and biotite and epidote have partially replaced the albite (Ab_{97}). The number of lath-like phenocrysts of albite increases at the exposed edges of the intrusive and a foliation is developed. Grain size of the feldspar laths increases in the

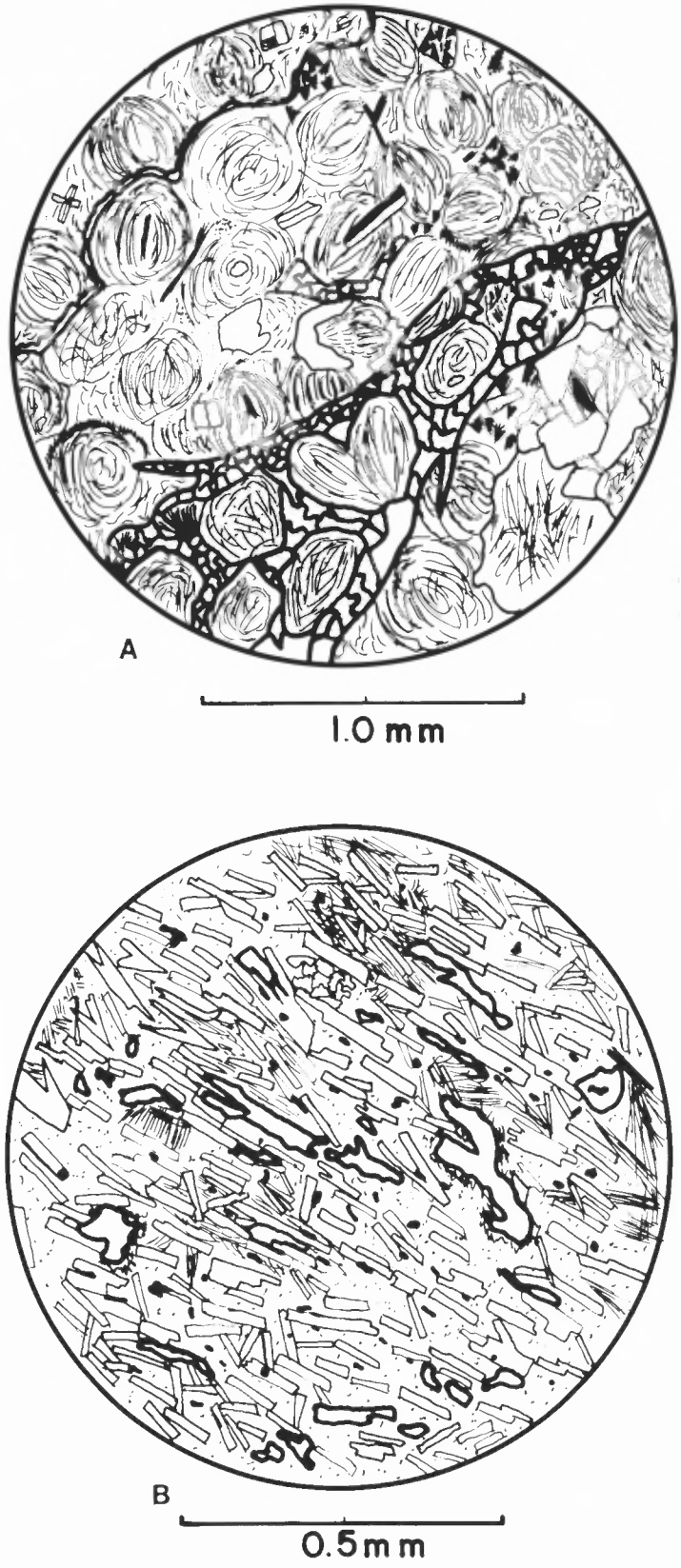

FIGURE 2—Composite sketches of textures in thin section. **A,** Spherulitic texture with resorbed quartz and granophyric feldspar and quartz, albite microphenocrysts, veinlets of epidote and biotite (higher-relief grains and fibers), and very fine-grained titanite (stippled). **B,** Trachytic texture. Lath-like albite essentially outlined by cryptocrystalline felsic intergrowths and Mg-rich calciferous amphibole (stippled). Fibrous mats of tremolite, titanite (heavy stipples and blebs), and epidote (high relief) are intergranular.

northern extension of the intrusive where it narrows to a sill or dike. Here, a trachytic texture is well developed and flow foliation can be seen in outcrop. The rock contains intergranular amphibole, titanite, epidote, and quartz. Small-scale fractures and veinlets of quartz, quartz–clinozoisite–biotite–titanite–hematite, and clinozoisite–piemontite(?)–zoisite are very common. Fluorite, vesuvianite, and unidentified opaque minerals also are in veinlets. Many of the veinlets completely enclose spherulites, particularly clinozoisite/piemontite/zoisite veinlets. Some veinlets occur in sinusoidal form as they wrap about spherulites (Fig. 2A). In places, veinlets physically resemble stylolites. In many samples, very fine-grained biotite and titanite are concentrated in diffuse zones on either side of veinlets and fractures. Autobrecciation has occurred locally along the margins of the intrusive, with titanite, biotite, and epidote concentrated around the edges of the breccia fragments.

Felsic mineral intergrowths

Samples either have no spherulites or between 30% and 95% of spherulites. The remaining percentage is made up mostly of felty felsic intergrowths and granophyric intergrowths. The composition of the spherulites is not well known because of the fine-grained nature. Spherulitic intergrowths of what is believed to be albite, quartz, and/or cristobalite average 0.15 mm in diameter and rarely reach 0.20 mm. Fibers of albite are concentric rather than radial and have commonly nucleated on spherical to oblate quartz grains or microphenocrysts of albite. Cryptocrystalline opaques, sericite, and biotite occur within the spherulitic growths; biotite, sericite, and albite microphenocrysts commonly extend outside of them into the interstitial area.

The conclusion that the spherulites consist of low-albite fibers with quartz and/or cristobalite between fibers is based on the following observations: (1) The negative index of refractions is low. (2) Microphenocrysts of plagioclase analyzed by a MAC 400S (EDS) microprobe were Ab_{95}–Ab_{97}. (3) Since spherulites could not be separated from the matrix, a whole-rock sample with 90% spherulitic crystallization was powdered and analyzed by x-ray diffraction, which indicated the presence of low-albite, quartz, and cristobalite. (4) No orthoclase or sanidine was indicated by the x-ray-diffraction pattern in this study. (5) Fibers in the spherulites remained unstained in thin sections stained for K or Ca plus other alkaline earth metals. (6) Experimentally produced spherulites were composed predominantly of alkali feldspars (Lofgren 1971). Cristobalite was intergrown with the feldspar in runs with molalities of alkali solutions less than 0.1 m.

Albite phenocrysts

Most albite phenocrysts (Tab. 1) are 0.1–0.45 mm in maximum dimension. The majority are euhedral, contain fluid inclusions, are only slightly altered, and are twinned and glomeroporphyritic. Some phenocrysts have been partially replaced by epidote and biotite.

Quartz

Quartz (0.01–1.5 mm) is euhedral in veinlets and miarolitic cavities, but rarely so in the matrix. It is generally interstitial to and within the cores of the spherulites. Micropoikilitic quartz grains in the matrix enclose or partially enclose spherulites and in places are subhedral prismatic. Grains in veinlets, cavities, and matrix contain fluid inclusions, many of which are aligned. Nearly circular chains of micropoikilitic quartz grains are common. In miarolitic cavities and veinlets, quartz rims epidote and vice versa. Much of the micropoikilitic quartz is polygonal with 120° grain boundaries. Some euhedral, hexagonal quartz grains were found in a matrix of clay, which is probably the end product of biotite recrystallization, or residual glass hydration. The hexagonal quartz has felty plagioclase growing from resorbed rims.

Epidote group

Zoisite, clinozoisite, epidote, and piemontite were identified petrographically. Grain size ranges from 0.01 mm in the matrix to 1.0 mm in cavities and veinlets. Qualitative chemical analyses were obtained by microprobe EDS. This group (herein referred to as epidote), like quartz and biotite, occurs in miarolitic cavities, in veinlets, and interstitial to spherulitic growths. Epidote (but not piemontite) is also pseudomorphic after, or partially replaces, feldspar and biotite. The interstitial epidote frequently occurs in radiating splays of prismatic grains. It is also complexly intergrown with biotite. The cores of some epidote may be allanite. Titanite commonly rims epidote grains.

TABLE 1—Microprobe analyses of plagioclase*

Sample number		67j	17a	17b
Weight percent				
SiO_2		69.3	67.0	67.61
Al_2O_3		19.8	20.6	20.8
TiO_2		0.0	0.0	0.0
CaO		0.5	0.2	0.1
Na_2O		11.3	11.3	11.3
K_2O		0.4	0.3	0.5
FeO		0.0	0.0	0.0
Total		101.3	99.3	99.8
Number of ions on the basis of 8 anions				
Si		3.0	2.9	2.9
Al		1.0	1.1	1.1
Ti		0.0	0.0	0.0
Ca		0.0	0.0	0.0
Na		1.0	1.0	1.0
K		0.0	0.0	0.0
Fe		0.0	0.0	0.0
Mol.%	Ab	0.95	0.97	0.97
	An	0.02	0.01	0.01
	Or	0.02	0.02	0.03

*energy dispersive system, MAC 400S, 15 KeV operating voltage, 50 second count times, orthoclase, albite,and bytownite standards; samples located on Fig. 1.

Biotite

Two generations of biotite are present, along with what is probably recrystallized biotite. Subhedral, dark-amber to brown, lath-like crystals are usually interstitial to spherulites but also occur within them. Straw-yellow, fibrous, often radial biotite commonly fills interstitial areas and is intergrown with epidote and titanite. Rarely, biotites in veinlets are blood-red and the color of biotite growing from the rims of albite microphenocrysts is green. Both types of biotite are strongly altered and range in size from 0.01 to 0.10 mm in maximum dimension. Laths of biotite are commonly replaced by epidote and titanite, i.e. one end of the grain is biotite, a central region is epidote, and the opposite end is titanite. Biotite also occurs in veinlets and miarolitic cavities, with epidote, quartz, and titanite.

Biotite analyses are presented in Tab. 2 and calculated compositions are shown in Fig. 3. Sample locations are shown in Fig. 1. The two altered biotites can usually be distinguished both petrographically and chemically. The brown lath-like biotites generally have higher analytical totals and more SiO_2 (higher number of Si ions/unit cell, Fig. 3) and K_2O (Tab. 2) than the straw-yellow fibrous biotites. On the average, Al_2O_3, SnO_2, and F are higher in the less-altered, lath-like biotites, and FeO, MnO, CaO, and Cl are higher in the more altered fibrous biotites. The more altered grains are more siderophyllic and a distinction between the two generations in each thin section is evident (Fig. 3). For sample 84-012 the dividing line is between 5.8 and 6.1 Si ions, for sample 84-058b between 5.7 and 5.8 ions; the division is less obvious for sample 84-015, but a line between 5.97 and 5.98 Si ions is supported by

TABLE 2—Representative WDS (wave-length dispersive spectrometry) microprobe analyses of altered biotites. Sample current (on brass) of 10 nanoamps, accelerating voltage of 15 KeV, count times of 20 seconds for peaks, 10 seconds for background, and the following standards: fluorophlogopite, Lemhi biotite, albite, orthoclase, diopside, synthetic barium sodium niobate, cassiterite, synthetic rutile, willemite, hematite, and spessartine. Analyses performed using an ARLSEMQ instrument with six automated WDS spectrometers (USGS, Denver, Colorado).

Sample No.	12*	12+	15*	15+	58b*	58b+
weight percent						
SiO_2	46.71	38.04	43.54	33.95	37.54	33.65
TiO_2	0.03	0.05	0.04	0.07	0.05	0.09
Al_2O_3	22.33	26.75	26.26	23.35	19.23	19.30
FeO	13.47	16.06	10.84	21.15	20.18	20.93
MnO	0.64	0.81	0.36	0.96	0.52	0.58
MgO	3.19	3.86	3.61	3.99	9.26	10.67
SnO_2	0.05	0.02	0.01	0.00	0.02	0.00
ZnO	0.20	0.07	0.04	0.15	0.13	0.09
CaO	0.07	0.09	0.24	0.37	0.22	0.14
Na_2O	0.16	0.07	0.08	0.06	0.07	0.06
K_2O	7.48	2.77	7.69	4.37	0.82	0.79
BaO	0.05	0.00	0.00	0.03	0.02	0.06
F	0.00	0.04	0.16	0.23	0.26	0.21
Cl	0.01	0.02	0.00	0.02	0.02	0.02
H_2O	4.21	3.94	4.11	3.62	3.72	3.62
	98.59	92.59	96.98	92.32	92.06	90.21
O=F,Cl	0.00	0.02	0.07	0.10	0.11	0.09
TOTAL	98.59	92.57	96.91	92.22	91.95	90.12
NUMBER OF IONS ON THE BASIS OF 24 ANIONS						
Si	6.642	5.761	6.237	5.448	5.849	5.433
Ti	0.003	0.005	0.004	0.009	0.006	0.010
Al	3.744	4.773	4.434	4.416	3.531	3.674
Fe	1.603	2.034	1.299	2.839	2.630	2.826
Mn	0.077	0.104	0.044	0.131	0.068	0.079
Mg	0.675	0.870	0.768	0.955	2.150	2.568
Sn	0.003	0.001	0.001	0.000	0.001	0.000
Zn	0.021	0.008	0.004	0.018	0.014	0.011
Ca	0.011	0.015	0.037	0.063	0.036	0.025
Na	0.044	0.021	0.022	0.018	0.022	0.018
K	1.357	0.534	1.405	0.894	0.163	0.163
Ba	0.003	0.000	0.000	0.002	0.001	0.004
F	0.000	0.021	0.074	0.117	0.128	0.101
Cl	0.003	0.006	0.001	0.006	0.004	0.006
OH	3.997	3.973	3.925	3.877	3.868	3.893

H_2O CONCENTRATION ADJUSTED TO 4-(F+CL) PER UNIT CELL

*high analytical totals and high # of Si ions in formulae
+low analytical totals and low # of Si ions in formulae

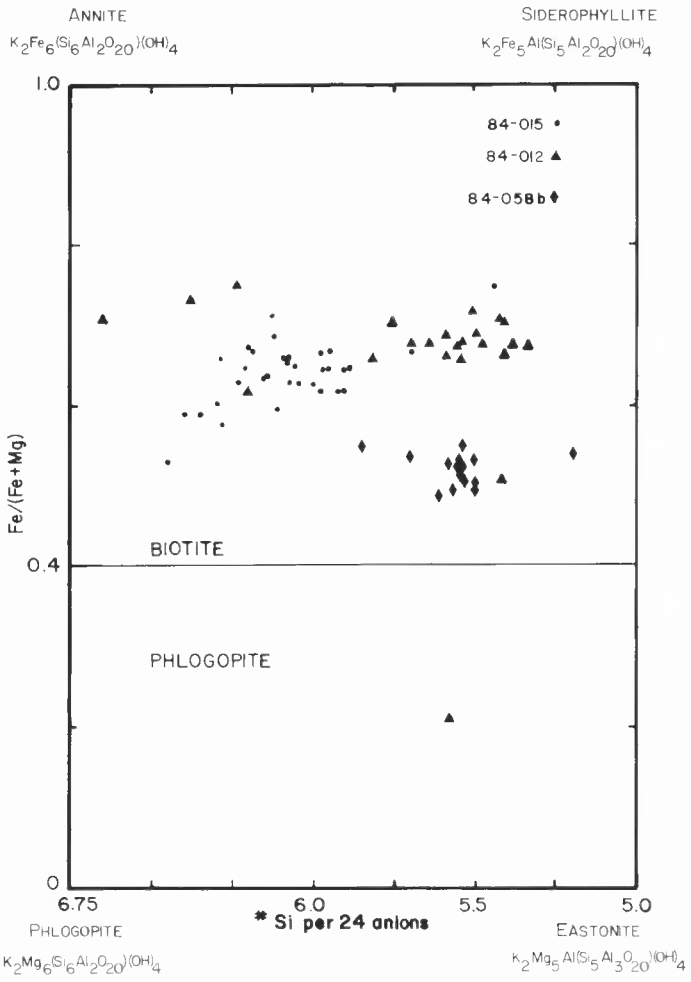

FIGURE 3—Microprobe compositions of altered biotite from main body of the high-silica intrusive rhyolite. Sample locations are shown in Fig. 1. See Tab. 2 for microprobe details.

analytical totals and petrography, i.e. lath-like biotites with relatively higher analytical totals lie to the left of this line. Inhomogeneity within grains is indicated by large variances in Al_2O_3, SiO_2, K_2O, MgO, and FeO and to a lesser degree ZnO, TiO_2, and MnO. These biotites are very similar to those studied by Hildreth (1977, 1979) and Keith (1982) that showed severe deficiencies in K_2O, low analytical totals, and addition of interlayer CaO and H_2O.

Titanite

Titanite (0.01 mm) typically occurs in fine-grained aggregates (0.05–0.80 mm), but also as euhedral rhombs. Microprobe analyses were needed for identification. Titanite aggregates are concentrated near veinlets, around breccia fragments, and in trachytic rocks. In some samples near exoskarn, titanite forms discontinuous stringers giving the rock a banded appearance. Euhedral rhombs often occur in veinlets with piemontite and epidote, whereas the granular aggregates are either alone or intergrown with epidote, biotite, and muscovite/sericite. Many have apparently opaque cores, probably rutile, Ti-magnetite or ilmenite, but morphology and small grain size prohibited a positive identification.

Sericite–mucovite–kaolinite

Some thin sections have approximately 14% combined kaolinite, sericite, and muscovite by volume. Muscovite/sericite grains are very difficult to distinguish from kaolinite. Muscovite that reaches 0.30 mm in size is easily distinguished. The cellular morphology of the kaolinite is distinctive, but the grain size usually prohibits identification. Several samples were stained for K. The muscovite did not take the stain while the kaolinite did, making a discrimination possible. When the grain size of both the muscovite/sericite and kaolinite is very fine a distinction is impossible, but some can be told by the manner of occurrence.

Muscovite rims biotite and spherulites. Some laths may be leached biotite rather than muscovite.

The kaolinite occurs as a fine "dusting" on almost all phases. Identification of kaolinite is tentative and it may be the same composition as (1) the very fine-grained clayey aggregates that biotite has been replaced by or recrystallized to, and (2) what may be devitrified or hydrated residual glass.

Other accessories

Apatite, magnetite, hematite, fluorite, vesuvianite, and unidentified opaques are present, but comprise less than 1% of the rock. Apatite, magnetite, and hematite are disseminated throughout the thin sections studied. The cryptocrystalline opaques within the spherulites may be entirely magnetite. Fluorite and vesuvianite were only found in veinlets. Mg-rich calciferous amphibole is present in the northern extension of the intrusion. Semiquantitative microprobe EDS analyses showed about 24% CaO and 15% MgO.

DISCUSSION

The spherulitic and granophyric morphology of the Reilly Peak intrusive indicates not only its very siliceous nature but gives clues to its

genesis. Lofgren (1971, 1974) experimentally produced similar textures in materials of similar chemical composition in two different ways: (1) isothermally at a substantial, constant, rapidly attained undercooling (ΔT), and (2) through devitrification of a quenched glass by adding alkaline solutions. A substance that remains liquid below the expected freezing point is said to be supercooled (= undercooled); the difference between the actual T of crystallization and the expected T of crystallization is ΔT. Drever et al. (1972) suggested that supercooling and quenching are not synonymous, and Hughes (1982) described two processes to explain the development of spherulites other than supercooling. They are: (1) changes in pressure (without any violent temperature quenching) such as that which would occur upon ascent of the magma, and (2) a loss of water. Textures in the Reilly Peak intrusive may have been produced by a large, constant ΔT that was rapidly attained or by devitrification of a quenched melt. It is important to note that the difference between a glass and a structured melt which would be produced by a large ΔT is small. Quartz, albite, lath-like biotite, and possibly titanite crystallized before the spherulites formed or at the same time. Lofgren (1980) suggested that textural variations within a few millimeters may just be the result of irregular distribution of nuclei.

The epidote and fibrous, straw-yellow biotite that grew in the interstitial areas after the development of the spherulites may have crystallized from a vapor phase. The interstitial epidote is primary and is not an alteration product. The large amount of Ca in both types of biotite (Tab. 2) may indicate a high Ca activity and may explain why epidote rather than aluminosilicates such as topaz crystallized (J.D. Keith oral comm. 1986). The miarolitic cavities in this study may be similar to what Lofgren (1971) thought were the result of the volume change that occurred due to the formation of spherulites. Two types of altered biotite, altered epidote, clay, and veinlets or healed fractures attest to several pulses of hydrothermal fluids. These fluids locally redistributed certain elements, e.g. K and Fe. H_2O and CaO were added to both the biotites with high analytical totals and a high number of Si ions per unit cell, and the biotites with low analytical totals and a low number of Si ions per unit cell (Tab. 2). K_2O and Na_2O were leached from both biotites as well.

Undercooling or quenching and alteration of the intrusive were not uniform. Spherulite concentration decreases from the central portion of the intrusive outwards. Hydrothermal alteration of the intrusive is reflected in the altered biotites. Biotites from three samples of the Reilly Peak intrusive were probed. Each sample contained two different species of biotite (Tab. 2) and each sample was significantly different from the other two samples (Fig. 3). This indicates that alteration events affected the intrusive inequally. Fractures, temperatures of fluids, and fluid composition all partially controlled the alteration.

The Reilly Peak intrusive is part of a much larger system. It may be a stock similar to the near-vertical digital protrusion from a larger igneous body as described by Gustafson & Hunt (1975). Alteration of the intrusive, tetrahedral fracturing of both intrusive and sedimentary rocks, very fine-scaled healed fractures, and the presence of endo- and exoskarn lead to several conclusions. The Reilly Peak intrusive and associated dikes baked the sedimentary rocks enough to form a metamorphic skarn and marble (Jahns 1944a, b). Pathways for fluids were opened by fracturing which began before and continued after emplacement of intrusive rocks. Fluids probably sealed off fractures episodically (Burnham 1979). Fluids also used contacts between intrusive rocks and sedimentary rocks as pathways. Biotite variation between samples probably reflects the episodic nature of fluid flow. Mineral assemblages within the exoskarn reflect several pulses of fluids (Jahns 1944a, b, Davis in preparation), e.g. several temperatures were obtained from fluid inclusions, mineral assemblages do not reflect equilibrium (Jahns 1944a, b, Jahns 1955, Davis in preparation), and both massive skarn and "ribbon rock" are present.

REFERENCES

Almins H.V., Watts K.C., Griffitts W.R., Siems D.L., Kraxberger V.E. & Curry K.J. 1975a. Map showing anomalous distribution of tungsten, fluorite, and silver in stream-sediment concentrates from the Sierra Cuchillo–Animas uplifts and adjacent areas, southwestern New Mexico.—U.S. Geological Survey, Map I-880, scale 1:48,000.

Alminas H.V., Watts K.C., Griffitts W.R., Siems D.L., Kraxberger V.E. & Curry K.J. 1975b. Map showing anomalous distribution of lead, tin, and bismuth in stream-sediment concentrates from the Sierra Cuchillo–Animas uplifts and adjacent areas, southwestern New Mexico.—U.S. Geological Survey, Map I-881, scale 1:48,000.

Alminas H.V., Watts K.C., Griffitts W.R., Siems D.L., Kraxberger V.E. & Curry K.J. 1975c. Map showing anomalous distribution of molybdenum, copper, and zinc in stream-sediment concentrates from the Sierra Cuchillo–Animas uplifts and adjacent areas, southwestern New Mexico.—U.S. Geological Survey, Map I-882, scale 1:48,000.

Burnham C.W. 1979. Magmas and hydrothermal fluids. *In* Barnes H.L. (ed.), Geochemistry of hydrothermal ore deposits.—John Wiley & Sons, New York, pp. 71–133.

Correa B. 1980. Fluorine and lithophile element mineralization in the Black Range and Sierra Cuchillo, New Mexico. *In* Burt D.M. (ed.), Uranium mineralization in fluorine-enriched volcanic rocks.—U.S. Department of Energy, Report GJBX-225(80): 459–494.

Drever H.I., Johnston R., Butler P. Jr. & Gibb F.G.F. 1972. Some textures in Apollo 12 lunar igneous rocks and in terrestrial analogs. *In* King E.A. (ed.), Proceedings of the third lunar science conference.—Massachusetts Institute of Technology Press, Cambridge, Massachusetts, pp. 171–184.

Gustafson L.B. & Hunt J.P. 1975. The porphyry copper deposit at El Salvador, Chile.—Economic Geology, 70: 161–168.

Harley G.T. 1934. The geology and ore deposits of Sierra County, New Mexico.—New Mexico Bureau of Mines & Mineral Resources, Bulletin 10: 220 pp.

Hildreth E.W. 1977. The magma chamber of the Bishop Tuff: gradients in temperature, pressure, and composition (Ph.D. thesis).—University of California, Berkeley, 328 pp.

Hildreth E.W. 1979. The Bishop Tuff: evidence for the origin of zonation in silicic magma chambers.—Geological Society of America, Special Paper 180: 43–75.

Hughes C.J. 1982. Igneous petrology.—Elsevier, Amsterdam, 155 pp.

Jahns R.H. 1944a. "Ribbon Rock," an unusual beryllium-bearing tactite.—Economic Geology, 39: 173–205.

Jahns R.H. 1944b. Beryllium and tungsten deposits of the Iron Mountain district, Sierra and Socorro Counties, New Mexico.—U.S. Geological Survey, Bulletin 945-C: 45–79.

Jahns R.H. 1955. Geology of the Sierra Cuchillo, New Mexico.—New Mexico Geological Society, Guidebook 6: 158–174.

Jahns R.H., McMillan D.K., O'Brient J.D. & Fisher D.L. 1978. Geologic section in the Sierra Cuchillo and flanking areas, Sierra and Socorro Counties, New Mexico.—New Mexico Geological Society, Special Publication 7: 130–138.

Keith J.D. 1982. Magmatic evolution of the Pine Grove porphyry molybdenum system, southwestern Utah (Ph.D. thesis).—University of Wisconsin, Madison, 246 pp.

Kelley V.C. 1955. Geologic map of the Sierra County region, New Mexico.—New Mexico Geological Society, Guidebook 6, pocket.

Lasky S.G. 1932. The ore deposits of Socorro County, New Mexico.—New Mexico Bureau of Mines & Mineral Resources, Bulletin 8: 141 pp.

Lofgren G. 1971. Experimentally produced devitrification textures in natural rhyolitic glass.—Geological Society of America, Bulletin, 82: 111–124.

Lofgren G. 1974. An experimental study of plagioclase crystal morphology: isothermal crystallization.—American Journal of Science, 274: 243–273.

Lofgren G. 1980. Experimental studies on the dynamic crystallization of silicate melts. *In* Hargraves R.B. (ed.), Physics of magmatic processes.—Princeton University Press, pp. 487–543.

Lowell J.D. & Guilbert J.M. 1970. Lateral and vertical alteration—mineralization zoning in porphyry ore deposits.—Economic Geology, 65: 373–408.

Smythe D.D. 1921. A contact metamorphic iron-ore deposit near Fairview, New Mexico.—Economic Geology, 16: 410–418.

Strock L.W. 1941. A new helvite locality—a possible beryllium deposit.—Economic Geology, 36: 748–751.

Schoolhouse in Dusty, 1983. Photo G.R. Osburn.